

## CHAPTER 4

### Parity detection using double correlation

#### 4.0 Introduction

The purpose of this chapter is to point out certain subtle features of the Knox-Thompson (KT) technique that are inconsequential in the triple correlation (TC) method. These special features of the KT method were missed in the previous work which dealt with a point source: dealt only with SNR for the  $R_u$ 's. SNR for any technique involves a factor that depends on the source structure  $S_u$  in addition to the SNR for the double correlation of the point source function (PSFDC). This dependence is not very dramatic in the case of TC. Consider a binary star (whose individual components are unresolved) with component's fluxes say  $N_1$  and  $N_2$  and separation  $b$ . In the case of binaries the only ambiguity that is left over after measuring the autocorrelation, is its parity (defined as the side of the brighter component). In chapter 2 we estimated SNR for parity of a binary using TC. Though the SNR for parity determined using TC depends on the fluxes it does not strongly depend on the binary separation  $b$  as long it is smaller than the seeing. In this chapter we show that SNR for the parity of the binary determined by using the double correlation (ie KT) method depends linearly on binary separation (for small separations compared to the seeing disk). As a consequence of this dependence KT has poorer SNR for parity detection (for binaries close to the resolution limit) than the TC **inspite** of it being a second order statistic (the advantage due to lower order statistics shows for magnitudes

fainter than  $18^m$ ). This result is contrary to the existing analytical calculations (which use a point source as a representative) and is supported by numerical simulations for complex sources by Beletik (1988)<sup>[11]</sup> who finds the KT method to have poorer SNR for complex sources than the TC method. In section 4.1 we present our analytical estimates for parity detection using the double correlation. Numerical results are presented in section 4.5.

#### 4.1 Parity detection using double correlation

Our motivation for considering parity detection using double correlation is as follows. The crucial point in the KT method is the limitation on AU viz  $\Delta u < \Delta u_{max} \sim r_0 / \lambda f$  where  $r_0$  is the Fried parameter and  $f$  is the focal length of the speckle imaging system. The pupil plane length scale  $r_0$  gives rise to the 'seeing' disk of size  $\delta = \lambda f / r_0$  in the focal plane. If  $r_0$  were zero then  $\Delta u_{max}$  would become zero rendering KT method useless. In the limit  $r_0 / D \rightarrow 0$  ( $D$  is telescope diameter) the focal plane pattern due to a point source will become stationary (statistically invariant under shifts) in the focal plane. If any process is stationary then the only nonzero double correlation is the power spectrum  $\langle I_u I_{-u} \rangle$ . This, of course, does not contain any phase information. In reality the finite size of seeing disk saves the situation by breaking stationarity in the focal plane. Note that the bispectrum is a special case of the most general triple correlation  $\langle I_u I_v I_w \rangle$  with  $w = -u - v$ ; and is meaningful even in the limit  $r_0 / D \rightarrow 0$ . For a binary (within an isoplanatic patch) the focal plane image consists of two similar speckle patterns

due to the two stars forming the binary. Different speckles due to the same star have uncorrelated intensities, however, for every speckle due to star 1 there is one speckle due to the star 2 which has the same relative intensity and separation as the true binary. Any information about the binary must come from these correlated pairs of speckles (otherwise one can be happy with the long exposure image). Above we argued that for KT to work a finite seeing disk is a must. The statistic of speckles change on the scale  $\delta$  of the seeing disk **and** this change must be felt by the correlated pairs of speckles with separation  $b$ . We therefore expect a small parameter  $b/\delta$  in front of SNR for parity detection using double correlation which goes to zero smoothly as  $b/\delta \rightarrow 0$ . This is confirmed in the detailed calculations given below. Before presenting them we give frequency domain arguments to show that this small parameter should also be present for SNR for phase determination for objects small compared to the seeing disk.

Frequency domain estimates

The double correlation used in KT method can be expanded in a Taylor series as follows:

$$\langle I_u I_{-u+\Delta u} \rangle = \langle I_u I_{-u} \rangle + \Delta u \cdot \langle R_u R_{-u} \rangle S_u \nabla S|_{-u} + \Delta u \cdot \langle R_u \nabla R|_{-u} \rangle S_u S_{-u} + O(\Delta u^2) \quad (4.1)$$

The first term is just the power spectrum  $\langle I_u I_{-u} \rangle$ . The third term contains only the power spectrum of the source and not its phase. Only the second term contains phase information. Also note that both the second and the third term depend on the choice of the origin in the focal plane through the gradient. Since the

second term contains phase information we show the origin dependence explicitly. Let the binary be

$$S(x) = \alpha_1 \delta(x-x_1) + \alpha_2 \delta(x-x_2) \text{ or } S_u = \alpha_1 e^{iux_1} + \alpha_2 e^{iux_2} \quad (4.2)$$

If  $b = x_2 - x_1$  is the binary separation then one can write the coordinates of the components as

$$x_1 = x_c - \frac{\alpha_2}{\alpha_1 + \alpha_2} b \quad ; \quad x_2 = x_c + \frac{\alpha_1}{\alpha_1 + \alpha_2} b \quad (4.3)$$

where  $x_c$  is the flux center of the binary:  $x_c = \frac{\alpha_1 x_1 + \alpha_2 x_2}{\alpha_1 + \alpha_2}$  With this the second term (apart from  $\langle R_u R_{-u} \rangle$ ) becomes

$$\begin{aligned} \Delta u \cdot S_u \nabla S|_{-u} = & i \Delta u \cdot x_c (\alpha_1^2 + \alpha_2^2 + 2\alpha_1 \alpha_2 \cos(ub)) + i \Delta u \cdot b \frac{\alpha_1 \alpha_2 (\alpha_1 - \alpha_2)}{\alpha_1 + \alpha_2} \\ & + i \frac{\alpha_1^2 \alpha_2}{\alpha_1 + \alpha_2} e^{-iub} \Delta u \cdot b - i \frac{\alpha_1 \alpha_2^2}{\alpha_1 + \alpha_2} e^{iub} \Delta u \cdot b \end{aligned} \quad (4.4)$$

Note that the coefficient of the flux center  $x_c$  is the power spectrum of the binary. In general, though the second term depends on the choice of the focal plane origin, the origin dependent contribution is the power spectrum. The KT signal proper comes when the flux center is chosen as the origin. Though the first term (usual power spectrum) in Eq 4.1 is noisy it is purely real by construction and cannot contaminate the purely imaginary part of the KT signal (for example the second term in Eq 4.4). The noise on this comes from the third term of Eq 4.1. Without any loss of generality, we choose the origin for the system response at the flux center so that in  $\Delta u \cdot \langle R_u \nabla R|_{-u} \rangle$  term analogous to the first in Eq 4.4 is absent.  $R_u$  and  $\nabla R_u$  can be treated as uncorrelated and thus  $\langle R_u \nabla R|_{-u} \rangle$  vanishes. However,  $\langle |R_u \nabla R_{-u}| \rangle \sim \frac{\langle R_u R_{-u} \rangle}{\Delta u_{max}}$  as  $\Delta u_{max}$  is correlation scale for  $R_u$ . Thus the noise on  $\langle R_u \nabla R_{-u} \rangle$  is the same as that for the usual power spectrum. We emphasize that the  $b$  dependence is true for all light levels: the SNR for KT method is  $\frac{b}{\delta}$  times poorer

than the corresponding SNR for the power spectrum method:

$$SNR_{PHASE(KT)} \sim (b/6) SNR_{POWER} \quad (4.5)$$

$$SNR_{PARITY(KT)} \sim (b/6) SNR_{AUTO} \quad (4.6)$$

Eq 4.6 follows from Eq 4.5 since information about the parity is contained in  $N_s \sim (\frac{D}{\lambda})^2$  independent phases:  $SNR_{PARITY} \sim N_s^{1/2} SNR_{PHASE}$  Similarly, autocorrelation is derived from  $N_s$  power spectrum values. Supplementing the above results by known results for autocorrelation method (Dainty 1974, Dainty et al 1979) we get for SNR of the KT method

$$SNR_{PHASE(KT)} \sim (b/6) \quad \text{high flux} \quad (4.7a)$$

$$\sim (b/6) \mathcal{N} \quad \text{low flux } \mathcal{N} < 1 \quad (4.7b)$$

$$SNR_{PARITY(KT)} \sim (b/6) N_s^{1/2} \quad \text{high flux} \quad (4.8a)$$

$$\sim (b/6) N_s^{1/2} \mathcal{N} \quad \text{low flux } \mathcal{N} < 1 \quad (4.8b)$$

where  $\mathcal{N}$  is photon count per speckle in an exposure. The factor  $\frac{b}{6}$  is about  $N_s^{-1/2}$  for binaries close to the resolution limit. For a 4 m telescope  $N_s^{-1/2} \sim \frac{1}{40}$ .

#### Focal plane calculations

In the following sections we support the frequency domain arguments given above by explicit analytic calculation of the SNR for parity detection using the double correlation. Our method is as follows. First we calculate the general double correlation (PSFDC) for the PSF which is inversion symmetric. The general double correlation for a binary is made of four PSFDCs. The strengths and locations of these four PSFDCs are asymmetric about the center of the binary double correlation. This leads to an asymmetry in the double correlation for the binary. This chapter

is aimed at locating those regions of the double correlation which contribute more to the asymmetry at the cost of minimum variance. To calculate PSFDC we need to assume the statistics obeyed by the pupil plane fields. We mimic atmospheric degradation by a single scale Gaussian correlation. In reality, departure from the single scale correlation is known to result in drifting centroids of the instantaneous speckle pattern. We discuss these issues later on in section 4.5. In this chapter we are not interested in correlation effects due to secondary Airy rings so use an apodized aperture to yield a Gaussian beam. The parity statistic (when defined) will be of the form

$$P = \int d^2x d^2y W(x,y) \langle I(x)I(y) \rangle \quad (4.9)$$

the sign of which tells us the parity of the binary. A near optimum choice of  $W$  is made so that SNR is (apart from numerical factors of the order unity) at its best. The parity signal, Eq 4.9, is second order in the intensity and is evaluated for the single scale Gaussian model described below. The variance of such a general double correlation involves terms second, third and fourth order in the intensity. In the case of the autocorrelation it is enough to consider only the lowest second order contribution if one is interested in "low" light levels (fainter than  $13^m$ ). Although it is obvious that even in the case of a general double correlation the second order terms should dominate at sufficiently "low" light levels it is not known a priori what "low" means for a specific choice of the weight function.

Consider an extreme example with  $W(X,Y)=1$  everywhere. The statistic in Eq 4.9 is just the square of the total flux through

the telescope. In this case there are two transitions before the second order contribution ultimately dominates. Since a sum of (independent) Poisson fluctuations is a Poisson distribution the total **photon** count  $N$  in a realization is a Poisson variable with mean  $\bar{N}$  the classical intensity for that realization. The unbiased estimator of the square of the flux is  $N(N-1)$ . Using the results derived in the third chapter we get the photonic variance

$$\bar{N}^4 + 4\bar{N}^3 + 2\bar{N}^2$$

The average over atmospheric fluctuations can be done approximately. Since the total flux is made up of a large number of independent Rayleigh fluctuations in the intensities of individual speckles we can treat the total flux as a Gaussian random variable with average  $N_s \mathcal{N}$  and standard deviation  $N_s^{1/2} \mathcal{N}$ . It can be shown that the SNR for the square of the total flux goes through two transitions:

$$\begin{array}{l}
 \text{One frame} \\
 M=1
 \end{array}
 \begin{array}{l}
 SNR_{FLUX^2} \sim \frac{1}{2} N_s^{1/2} \\
 \sim \frac{1}{2} N_s^{1/2} \mathcal{N}^{1/2} \mathcal{N}^{1/2} \\
 \sim \frac{1}{\sqrt{2}} N_s \mathcal{N}
 \end{array}
 \begin{array}{l}
 \downarrow \text{first transition } 4g\mathcal{N} = 1 \\
 \downarrow \text{second transition } 2gN_s\mathcal{N} = 1
 \end{array}$$

Below we show that the PSFDC contains two features A and B. Both these features are capable of yielding parity information. The feature B, which is also the basis of the autocorrelation analysis, yields parity with better SNR than the feature A (basically long exposure). For feature A there are two transitions in the flux levels. Since the parity detection due to the feature B has better SNR and "low" flux means fainter than  $13^m$  for this feature we calculate only the lowest second order

variance in this case. The calculation is based on a single scale Gaussian model for the pupil plane fields. The case of parity due to the feature A, is described here for the sake of completeness (it proves to be unimportant for high resolution imaging), needs variance calculation in all orders and is treated using the following approximations. First of all, we use the pixel model of the PSF described in section 2.1. This avoids the complexities of handling high order pupil plane field correlations. The second simplification is to let the binary shrink to a point. This is justified for the variance calculations (not for the signal). If the two components have widely different strengths then the noise, anyway, comes from the brighter source. In the more general case letting the binary shrink to a point neglects terms  $b/\delta$  times smaller than the leading terms. The type A term is important for binary separations of the order of the seeing disk.

#### 4.2 The PSFDC

In Fig 4.1 the double correlation for PSF is shown in the  $(Y_1, Z_1)$  plane. It consists of two features. The feature A has extension of the order of the seeing disk while the feature B is along the diagonal line  $X=Y$  with a width of the order of the speckle size and length of the order of the seeing disk. In the full four dimensional  $\chi$ - $\gamma$  space the feature A is a four sphere while the feature B is a two dimensional layer. In our Gaussian model all these features have Gaussian fall offs with the above mentioned length scales. In the figure, however, the features are shown more like a step for clarity of depiction. The two features have the same strength at the origin that can be readily



estimated. With our normalization  $\pi N_0 R^2$  is the total photon count per exposure for a zeroth magnitude star. This is distributed over the entire seeing disk of extent  $\delta = f/k\ell$ . Thus the average intensity density is  $N_0 k^2 \ell^2 R^2 / f^2$ . The general double correlation depicted in Fig 4.1 correlates intensity at two points in the focal plane. Now if these two points are separated more than a speckle size then their intensity fluctuations will be independent. For these regions the double correlation density will be the product of the individual intensity densities. This is the reason for the term A whose strength is therefore  $N_0^2 k^4 \ell^4 R^4 / f^4$ .

Note that this feature is meaningful even for a long exposure image. Now consider those regions of the double correlation where the two points involved in the correlation are within a speckle size. This region is specified by the plane  $X=Y$  with a tolerance of the speckle size. The intensity at these two points is correlated and therefore in this region there is excess correlation in addition to the term A. This **excess** is the term B. Note that this feature is a genuine high resolution feature: it does not exist for a long exposure image. The feature A represents the long exposure image while the feature B represents information coming from correlated pairs of speckles.

The double correlation for the binary is shown in Fig 4.2. Note that it contains four units of PSF double correlations with strengths and locations shown in Fig 4.2. Because of the asymmetry in their strengths and locations with respect to the center of the double correlation the binary double correlation is

asymmetric and one has to identify those regions of the double correlation which contribute significantly to the asymmetry. A more interesting question is to ask the relative importance of the two features of the **PSF** in determining the parity of the binary. The answer to this question has implications for the more general question of optimum weight function. Intuitively one expects the optimum weight function to have two domains: one each for the two features of the **PSFDC**. The relative weight of the two domains determines what fraction of information is obtained from a specific feature. So one should, in principle, consider a weight function with two domains whose relative weights are such that the SNR for the resulting parity statistics is maximum. However, it is not necessary to carry out such a parametric optimization. A kind of superposition approximation holds for the signal and the variance (but not for the **SNR** of course). Imagine that one knows the signal and the noise for the two features individually. Then the signal and the variance for any linear combination of the two features will be (approximately) the same linear combination of the appropriate quantities for the individual features. This simplification owes its existence to the fact that the features A and B have vastly different **four-**volumes. If we take the four volume of the feature B as unity then the four volume of the feature A is about  $N_s = 2000$ . For this reason, the difference between signal and noise due to the feature A and the feature A with voids of the size of the feature B is negligible. It turns out that for binary separation small compared to the seeing the feature B dominates while for separations comparable to the seeing the feature A dominates. So

we consider two kinds of weight functions: one designed to emphasize the feature B and the second to emphasize the feature A. We give the order of magnitude scalings below while the details are left to the appendix A4.

#### 4.3 SNR for parity detection using feature B:

In Fig 4.2 we have taken the star 1 as the origin in the focal plane. We have aligned the axes so that the binary lies along the first axis. The center of the entire double correlation  $(X_{c1}, X_{c2}, Y_{c1}, Y_{c2})$  is the same as the flux center of the long exposure image (double correlation is, of course, four dimensional but for the planes  $(X_1, Y_1)$  and  $(X_2, Y_2)$  the center coordinates are the same as the long exposure image i.e.  $X_{c1} = Y_{c1} = \frac{\alpha_2 b}{\alpha_1 + \alpha_2}$ ,  $X_{c2} = Y_{c2} = 0$ ). The center of the double correlation is shown by a cross in Fig 4.2. It is closer to the brighter star which we take to be the star 1. We note from the Fig 4.2 that the correlation ridges (feature B) appear along three strips, labeled  $S_1, S_2$  and  $S_3$  in Fig 4.2, in the  $(X, Y)$  plane. So our first choice of weight function which emphasizes the feature B is one which is nonzero only **along** these three strips. The weight function is shown in Fig 4.3. The strips have equivalent width that of the feature B. The asymmetry in the double correlation about the flux center can be considered as asymmetry in the individual strips about a  $-45^\circ$  line passing through the flux center. This is because the middle strip passes through the flux center and therefore its one side on inversion through the center becomes the other. However, the upper part of the strip 1 becomes the lower part of the strip 3 on inversion through the center. But the strips 1 and 3 are identical in all

realizations so lower part of the strip 3 can be replaced by the same that of strip 1. Thus one can talk of **asymmetry** of various  $+45^\circ$  strips about the  $-45^\circ$  line passing through the center of the double correlation. The middle correlation strip has its center displaced towards the brighter component of the binary while the other two strips have their centers shifted towards the fainter component by half the amount of the middle strip. For any other  $45^\circ$ -strip consisting only of feature A the center of the strip deviates from the  $-45^\circ$  line in third order in the binary separation and thus neglected for small separations. This motivates our weight function shown in Fig 4.3. In this and the next chapter we have considered representative weight functions which take only three values:  $-1, 0$  and  $1$ . In all figures the sign of the weight function is shown whenever it is nonzero.

Two points need to be clarified. The first point to note is that by definition the double correlation is symmetric in X and Y for every realization of the atmospheric and photonic noise. Therefore, the strips 1 and 3 are identical and do not contain independent information. Our weight function, however, does draw information from both these strips. As the following argument shows the SNR would have been the same if we had restricted the weight function to one side of the X=Y plane. We show this for low light levels which are relevant for this feature. At low light levels the variance for the double correlation, Eq 4.9, is given by

$$\int d^2x d^2y W(x,y) [W(x,y) + W(y,x)] \langle I(x)I(y) \rangle \quad (4.10)$$

Now consider a weight function W which is symmetric in X and Y

like our weight function in Fig 4.3. Then the variance is given by

$$V = 2 \int d^2x d^2y W^2(x,y) \langle I(x)I(y) \rangle \quad (4.11)$$

Now consider a weight function  $W_+$  which is obtained from  $W$  by retaining only the upper half of it

$$W_+(x,y) = W(x,y) \quad \text{if } y_1 > x_1 \\ = 0 \quad \text{otherwise}$$

It is obvious that for this weight function the signal  $S_+$  is half of the signal  $S$  for the weight function  $W$ :  $S_+ = 0.5 S$ . Since there is no overlap of  $W_+(X,Y)$  and  $W_+(Y,X)$  only one term in Eq 4.10 contributes to the variance and that too half of what it would for  $W$ :

$$V_+ = \int d^2x d^2y W_+^2(x,y) \langle I(x)I(y) \rangle = \frac{1}{2} \int d^2x d^2y W^2(x,y) \langle I(x)I(y) \rangle = \frac{1}{4} V$$

Thus the SNR for  $W_+$  and  $W$  is the same. Further it makes no simplification to favour  $W_+$  which involves integrals for the middle strip split halfway. The second point to be noted is that the strips 1 and 2 come with the same weight. Actually one should weigh the strips differently and work out the SNR for a choice of the relative weight. The relative weight is to be chosen so that the SNR is maximum. This question is best answered for  $W_+$ . The signal due to the strip 1 is equal to the signal due to the upper half of the strip 2. The variance due to the strip 1 and the upper half of the middle strip is  $\alpha_1^2 + 3\alpha_1\alpha_2 + \alpha_2^2$  and  $\alpha_1^2 + \alpha_1\alpha_2 + \alpha_2^2$  respectively in proper units. The difference in the variance is not alarming especially when one is interested in binaries with widely differing strengths. It is well known that if two independent variables estimate the same quantity then the best linear combination is the one which weighs the two variable by

the reciprocal of their variances. Since the variances for all the strips are nearly the same we consider equal weights for simplicity.

Although the weight function is designed to emphasis feature B it cannot filter out the all pervading term A which contributes mainly to the noise. It is shown in the appendix A4 that the parity signal from all the three strips is

$$S_B = \frac{\pi^{1.5} N_0^2 k l^3 R^2 b \alpha_1 \alpha_2 (\alpha_1 - \alpha_2)}{2^{3.5} f (\alpha_1 + \alpha_2)} \quad (4.11a)$$

The low light level variance is

$$V_B = \frac{1}{2} \pi^2 N_0^2 l^2 R^2 (\alpha_1 + \alpha_2)^2 \quad (4.11b)$$

Thus our estimate for the SNR for parity detection using the feature B is

$$SNR_{PARITY(KT/B)} = \frac{4}{\sqrt{\pi}} q M^{1/2} \frac{N_1 N_2 (N_1 - N_2)}{(N_1 + N_2)^2} B \quad (4.12)$$

where  $N = \frac{\pi l^2 N_0 \alpha}{16}$  is photon count per speckle in an exposure,  $B = \frac{k R b}{2f}$  is the binary separation in units of diameter  $\rho = \frac{2f}{kR}$  of the PSF in the absence of atmospheric noise,  $q$  is detector quantum efficiency and  $M$  is the number of frames of data used. As noted before the cause of the asymmetry is that the four PSFDCs are asymmetrically distributed about the center. If the four PSFDCs are taken futher apart then the asymmetry will increase, This is the reason why SNR depends on the binary separation. It may appear that only a fraction  $\frac{b}{\phi}$  of the strips contribute to the signal. This is not true: for example the signal density along the central strip is (apart from overall strength) of the form

$$S(\eta) \propto \eta \exp\left\{-\frac{k^2 l^2}{8 f^2} \eta^2\right\} \quad (4.13)$$

where  $\eta$  is the coordinate along the strip. The signal density is obtained by taking the difference between the double correlation values at two points  $\pm\eta$  away from the center of the strip. So the signal comes from all parts of the strip. If it were coming from some localized region then one could improve the SNR by restricting the weight function to this area thus cutting down noise from regions with no or little signal. Thus the weight function chosen is near optimum and one can improve SNR only slightly by fine tuning the weight function; the scalings with  $b$  or  $w$ 't be affected.

In autocorrelation analysis one is interested in getting the binary separation so one integrates along all  $45^\circ$ -strips. For the correlation strips the result will stand out relative to its neighbours.

#### 4.4 SNR for parity detection using feature A

Now we consider the asymmetry due to the uncorrelated regions of the double correlation. A representative weight function is shown in Fig 4.4. As mentioned before the contribution to asymmetry is in the third order in the binary separation. A straightforward calculation gives the parity contribution for this weight function:

$$S_A = \frac{\pi^{1.5}}{3 \cdot 2^{4.5}} N_0^2 \frac{k^3 l^3 R^4}{f^3} \frac{b^3}{b} \frac{\left\{ \alpha_1^2 \alpha_2^2 (\alpha_1 - \alpha_2) + \frac{1}{4} \alpha_1 \alpha_2 (\alpha_1 - \alpha_2)^2 \right\}}{(\alpha_1 + \alpha_2)^3} \quad (4.14)$$

However, the noise calculation is not very straightforward

because in the context of general weight function the term "low flux" needs qualification. In the following we derive an expression for the variance of a general double correlation valid for all light levels. Then we show that for autocorrelation (as is well known) and for the weight function used in the previous section low light levels indeed mean per speckle photon count in an exposure less than unity. For the weight function of the second kind considered in this section the variance is obtained in all orders. Consider, then, a general second order statistic

$$\sum W_{ij} \bar{\eta}_i \bar{\eta}_j \quad (4.15)$$

where  $\bar{\eta}_i$  is the intensity on the  $i$ 'th pixel. The noise on this statistics involves intensity correlations of second, third and fourth order. The lowest second order contribution is already given in Eq 4.10. This is what is ultimately relevant in the case of fainter and fainter objects. For brighter objects the fourth order contribution dominates. This is just the classical variance. The intermediate third order contribution should be relevant only in the transitional regime. In order to avoid the task of dealing with field correlations of rather **high** order we use the PSF model of section 2.1. Another simplifying factor is that while considering the variance one can take a point source as representative. In the case of the parity signal it was essential to consider the binary nature: the signal being in the first order in the separation. This is not so for the variance. The variance does not depend on the binary separation in its leading term. In the notation of chapter 2 the pixel **intensity**  $\bar{\eta}_i$ .



is made of two speckles

$$\bar{n}_i = \mu_i + \alpha \mu_{i-b}, \quad \alpha = \frac{W_2}{W_1} = \frac{\alpha_2}{\alpha_1} \quad (2.4)$$

where  $\mu_i$ 's are independent Rayleigh variables. Let us begin with classical fourth order contribution to the variance. The square of the statistics in Eq 4.15 is given by

$$\begin{aligned} \sum_{ijkl} W_{ij} W_{kl} \langle \bar{n}_i \bar{n}_j \bar{n}_k \bar{n}_l \rangle &= \sum_{ijkl} \langle \mu_i \mu_j \mu_k \mu_l \rangle \{ W_{ij} W_{kl} + \alpha^4 W_{i+bj+b} W_{k+b l+b} \\ &+ \alpha [ W_{ij} W_{k l+b} + W_{ij} W_{k+b l} + W_{ij+b} W_{kl} + W_{i+bj} W_{kl} ] \\ &+ \alpha^2 [ W_{i+bj+b} W_{kl} + W_{i+bj} W_{k+b l} + W_{i+bj} W_{k l+b} \\ &+ W_{ij+b} W_{k+b l} + W_{ij+b} W_{k l+b} + W_{ij} W_{k+b l+b} ] \\ &+ \alpha^3 [ W_{ij+b} W_{k+b l+b} + W_{i+bj} W_{k+b l+b} + W_{i+bj+b} W_{k l+b} + W_{i+bj+b} W_{k+b l} ] \} \end{aligned} \quad (4.16)$$

Since the four point intensity correlation does not vary much (by orders of magnitude) on the scale of the binary separation, for noise consideration, one can let  $b=0$  in the above expression. This reduces the number of terms to just one with appropriate weight:

$$\sum_{ijkl} W_{ij} W_{kl} \langle \bar{n}_i \bar{n}_j \bar{n}_k \bar{n}_l \rangle = (1+\alpha)^4 \sum_{ijkl} W_{ij} W_{kl} \langle \mu_i \mu_j \mu_k \mu_l \rangle \quad (4.17)$$

The classical variance is given by

$$V_4 = (1+\alpha)^4 \sum_{ijkl} W_{ij} W_{kl} [ \langle \mu_i \mu_j \mu_k \mu_l \rangle - \langle \mu_i \mu_j \rangle \langle \mu_k \mu_l \rangle ] \quad (4.18)$$

For the statistical model for the  $\mu$ 's (section 2.1) the fourth order correlation  $\langle \mu_i \mu_j \mu_k \mu_l \rangle$  can be shown to be

$$\begin{aligned} \langle \mu_i \mu_j \mu_k \mu_l \rangle &= \langle \mu_i \rangle \langle \mu_j \rangle \langle \mu_k \rangle \langle \mu_l \rangle + \delta_{ij} \langle \mu_i \rangle^2 \langle \mu_k \rangle \langle \mu_l \rangle + \delta_{ik} \langle \mu_i \rangle^2 \langle \mu_j \rangle \langle \mu_l \rangle \\ &+ \delta_{il} \langle \mu_i \rangle^2 \langle \mu_j \rangle \langle \mu_k \rangle + \delta_{jk} \langle \mu_i \rangle \langle \mu_j \rangle^2 \langle \mu_l \rangle + \delta_{jl} \langle \mu_i \rangle \langle \mu_j \rangle^2 \langle \mu_k \rangle \end{aligned}$$

$$\begin{aligned}
& + \delta_{kl} \langle \mu_i \rangle \langle \mu_j \rangle \langle \mu_k \rangle^2 + \delta_{ij} \delta_{kl} \langle \mu_i \rangle^2 \langle \mu_k \rangle^2 + \delta_{ik} \delta_{jl} \langle \mu_i \rangle^2 \langle \mu_j \rangle^2 \\
& + \delta_{il} \delta_{jk} \langle \mu_i \rangle^2 \langle \mu_j \rangle^2 + 2 \delta_{jkl} \langle \mu_i \rangle \langle \mu_j \rangle^3 + 2 \delta_{ikl} \langle \mu_i \rangle^3 \langle \mu_j \rangle \\
& + 2 \delta_{ijl} \langle \mu_i \rangle^3 \langle \mu_k \rangle + 2 \delta_{ijk} \langle \mu_i \rangle^3 \langle \mu_l \rangle + 6 \delta_{ijkl} \langle \mu_i \rangle^4
\end{aligned} \tag{4.19}$$

From this one must subtract the square of the mean

$$\begin{aligned}
\langle \mu_i \mu_j \rangle \langle \mu_k \mu_l \rangle = & \langle \mu_i \rangle \langle \mu_j \rangle \langle \mu_k \rangle \langle \mu_l \rangle + \delta_{ij} \langle \mu_i \rangle^2 \langle \mu_k \rangle \langle \mu_l \rangle + \delta_{kl} \langle \mu_i \rangle \langle \mu_j \rangle \langle \mu_k \rangle^2 \\
& + \delta_{ij} \delta_{kl} \langle \mu_i \rangle^2 \langle \mu_k \rangle^2
\end{aligned} \tag{4.20}$$

to get the variance:

$$\begin{aligned}
V_4 = & 8 \sum_{ijk} W_{ij} W_{ik} \langle \mu_i \rangle^2 \langle \mu_j \rangle \langle \mu_k \rangle + 4 \sum_{ij} W_{ij} (W_{ij} + W_{ji}) \langle \mu_i \rangle^2 \langle \mu_j \rangle^2 \\
& + 8 \sum_{ij} W_{ij} W_{ii} \langle \mu_i \rangle^3 \langle \mu_j \rangle + 6 \sum_{ii} W_{ii}^2 \langle \mu_i \rangle^4
\end{aligned} \tag{4.21}$$

In deriving Eq 4.21 from Eq 4.17 and (Eq 4.19-Eq 4.20) the symmetric nature of the W's used in this chapter and the fact that two W's appear was used.

We consider two kinds of weight functions. The first one covers the case of the autocorrelation and the one considered before stressing the feature B in parity detection:

$$\text{First kind} \quad W_{ij} = f_i \delta_{ij} \tag{4.22}$$

For this weight function all the terms in the variance are of the form  $N_s \mathcal{N}^4$ . It will be shown later that the third order contribution is of the form  $N_s \mathcal{N}^3$ . We have seen above that the second order contribution for this weight function is  $N_s \mathcal{N}^2$ . Thus for weight functions of this kind low flux means  $\mathcal{N} < 1$  i.e. fainter than  $13^m$ .

Now consider the weight function of the second kind shown in

Fig 4.4 . The discrete analogue of which is

$$\text{Second kind } W_{i_1 i_2 j_1 j_2} = \text{sign}[i_1 + j_1] \quad (4.23)$$

where we have written the vector subscript  $i$  in terms of its components and chosen  $i_1$  to be along the binary. The components run from  $-\frac{N_s^{1/2}}{2}$  to  $+\frac{N_s^{1/2}}{2}$ . The **restriction** actually comes from the fact that all intensity correlations extend only **upto** the seeing disk. In the spirit of the second chapter all correlations are treated constant inside the seeing disk and the limitation in the extension is taken up by the indices. For this weight function it can be shown that

$$\sum_{j_1, j_2, i_2} W_{i_1 i_2 j_1 j_2} = 2 i_1 N_s \quad (4.24)$$

The case is similar to one shown in Fig 5.5 after summing over  $i_2$  and  $j_2$  which just gives  $N_s$  as  $W$  does not depend on these indices. Thus the fourth order contribution to the variance is

$$(1+\alpha)^4 \left[ \frac{8}{3} N_s^3 \mathcal{N}^4 + 12 N_s^2 \mathcal{N}^4 + 6 N_s \mathcal{N}^4 \right] \sim (1+\alpha)^4 \frac{8}{3} N_s^3 \mathcal{N}^4 \quad (4.25)$$

As an application of the results derived in chapter 3 on Poisson fluctuations and using the symmetry of the weight function together with the fact that two  $W$ 's appear we get the third order contribution to the variance of a general double correlation:

$$V_3 = 4(1+\alpha)^3 \sum_{ijk} W_{ij} W_{ik} \left[ \langle \mu_i \rangle \langle \mu_j \rangle \langle \mu_k \rangle + \delta_{ij} \langle \mu_i \rangle^2 \langle \mu_k \rangle + \delta_{ik} \langle \mu_i \rangle^2 \langle \mu_j \rangle + \delta_{jk} \langle \mu_i \rangle \langle \mu_j \rangle^2 + 2 \delta_{ijk} \langle \mu_i \rangle^3 \right]$$

Note that for the weight function of the first kind all terms are of the form  $N_s \mathcal{N}^3$ . Coming back to the weight function of the second kind we get the third order variance

$$(1+\alpha)^3 \mathcal{N}^3 \left[ \frac{4}{3} N_s^3 + 8 N_s^2 + 8 N_s \right] \sim \frac{4}{3} (1+\alpha)^3 N_s^3 \mathcal{N}^3 \quad (4.26)$$

The second order contribution is of the form

$$2(1+\alpha)^2 \mathcal{N}^2 (N_s^2 + N_s) \sim 2(1+\alpha)^2 N_s^2 \mathcal{N}^2 \quad (4.27)$$

For this weight function there are two transition regions. The first one is when the dominant variance comes from the third order terms instead of the classical fourth order which dominate for bright sources. This happens for objects between  $13^m$  and  $19^m$ . The second transition occurs when the total flux is less than unity. The second order terms take over finally. The SNR for parity detection using the feature A is given by

$$SNR_{KT/A} = \frac{8}{\sqrt{3\pi}} \frac{M^{1/2}}{N_s} \frac{\mathcal{N}_1^2 \mathcal{N}_2^2 (\mathcal{N}_1 - \mathcal{N}_2) + \frac{1}{2} \mathcal{N}_1 \mathcal{N}_2 (\mathcal{N}_1 - \mathcal{N}_2)^2}{(\mathcal{N}_1 + \mathcal{N}_2)^5} \mathcal{B}^3 \quad \text{high flux} \quad (4.28a)$$

$$= \frac{8\sqrt{2}}{\sqrt{3\pi}} \frac{q^{1/2} M^{1/2}}{N_s} \frac{\mathcal{N}_1^2 \mathcal{N}_2^2 (\mathcal{N}_1 - \mathcal{N}_2) + \frac{1}{2} \mathcal{N}_1 \mathcal{N}_2 (\mathcal{N}_1 - \mathcal{N}_2)^2}{(\mathcal{N}_1 + \mathcal{N}_2)^{4.5}} \mathcal{B}^3 \quad \text{medium flux} \quad (4.28b)$$

$$= \frac{16}{3\sqrt{\pi}} \frac{q M^{1/2}}{N_s^{1/2}} \frac{\mathcal{N}_1^2 \mathcal{N}_2^2 (\mathcal{N}_1 - \mathcal{N}_2) + \frac{1}{2} \mathcal{N}_1 \mathcal{N}_2 (\mathcal{N}_1 - \mathcal{N}_2)^2}{(\mathcal{N}_1 + \mathcal{N}_2)^4} \mathcal{B}^3 \quad \text{low flux} \quad (4.28c)$$

One can ask the following question. For given brightness of the source what is the binary separation beyond which the parity is better determined by the feature A than the feature B. We do this for a typical binary:  $\mathcal{N}_2 = \frac{1}{2} \mathcal{N}_1$ ,  $\mathcal{N}_1 - \mathcal{N}_2 = \frac{1}{2} \mathcal{N}_1$ . (This binary is expected to have better SNR as almost all SNR expressions have  $\mathcal{N}_1 \mathcal{N}_2 (\mathcal{N}_1 - \mathcal{N}_2)$  in the numerator). Equating the two expressions for the SNR we find this separation to be

$$\mathcal{B} = \frac{3}{2} q^{1/4} N_s^{1/2} \mathcal{N}^{1/4} \quad (4.29)$$

This formula is valid for  $2q\mathcal{N} < 1$  (as we have used 'low' flux calculations for the feature B) and  $\frac{2}{3}qN_s\mathcal{N} > 1$  (as we use 'medium' flux variance for the feature A). When  $\mathcal{N} = 1$  we get  $\mathcal{B} = N_s^{1/2}$  i.e. the separation is equal to the seeing disk (this is a rather risky extrapolation of the Taylored calculations). As  $\mathcal{N}$  reduces the

binary separation for which the two features contribute equally also decreases. For a 4 m telescope,  $q=0.2$ , we have given in table 4.1 the values of  $\mathcal{B}$  beyond which long exposure feature A determines the parity better than the high resolution feature B.

Table 4.1 Binary separations beyond which the feature A has a better SNR than the feature B

Magnitude	14	15	16	17	18	19
Separation $\mathcal{B}$	34	26	21	17	13	10

The feature A in the double correlation represents uncorrelated fluctuations in the intensities of the two points for which the double correlation is considered. So the weight function under consideration is actually dealing with a long exposure image. To see this more clearly we write

$$\sum_{i,j} W_{ij} \langle \bar{n}_i \bar{n}_j \rangle = \sum_{\substack{j \neq i \\ \neq i \pm b}} W_{ij} \langle \bar{n}_i \rangle \langle \bar{n}_j \rangle + \sum_i W_{ii} \langle \bar{n}_i^2 \rangle + 2 \sum_i W_{i,i+b} \langle \bar{n}_i \bar{n}_{i+b} \rangle \quad (4.30)$$

The last two terms represent contribution due to correlation ridges. For separations larger than those given in the table 4.1 the last two terms are negligible. The first term contains  $\bar{n}_i$  and  $\bar{n}_j$  which are uncorrelated as the separation between the pixels is different from the binary separation. Thus the average is

$$\sum W_{ij} \langle \bar{n}_i \bar{n}_j \rangle \sim \sum W_{ij} \langle \bar{n}_i \rangle \langle \bar{n}_j \rangle \quad (4.31)$$

We can think of this as equivalent to a first order statistics

$$\sum f_i \bar{n}_i \quad (4.32a)$$

where the equivalent weight function  $f_i$  is given by

$$f_i = \sum_j W_{ij} \bar{n}_j \quad (4.32b)$$

Now, if we go to the flux center of the long exposure binary image then a constant weight function would give the total flux; a linear weight function gives zero (by the definition of the flux center); a parabolic weight function gives the width of the image and thus can tell about the binary nature; a cubic weight function gives the parity. Now since  $w_{ij}$  is inversion antisymmetric  $f_i = \sum_j w_{ij} \bar{n}_j$  contains only odd powers of  $i_1$  in the average sense. So we see that our weight function is essentially playing the role of an equivalent weight function  $i_1^3$  in the case of first order parity statistics. In fact it is worse than that. The equivalent function has fluctuating nature as apposed to  $i_1^3$ , which is deterministic. In the specific case of binary stars the feature A may have larger SNR for large separations but it cannot be considered as a truly high resolution feature: for more complicated sources with fine structure only feature B is of any relevance.

#### 4.5 Numerical results and discussion

In this section we present numerical results for the SNR for parity detection using double correlation. We are concerned only with the SNR due to the correlation ridges which, as argued before, are the true high resolution information carriers. First of all letting  $\mathcal{N}_2 = \mathcal{N}_1 - \mathcal{N}_2 = \frac{\mathcal{N}_1}{2}$  we see that for reasonable observational parameters (10 ms exposure,  $10^5$  frames, 100 A bandwidth and detection efficiency 0.2) a SNR of 3 can be achieved for objects brighter than  $14^m$  for separations close to the resolution limit. Also note from the SNR expression Eq 4.12 that the SNR

(for fixed  $\mathcal{B}$ ) is independent of the telescope diameter. This is because of the small factor  $\frac{b}{a}$  which masks the usual  $N_s^{1/2}$  factor in the SNR. If in any technique individual speckles carry information then there is a factor  $N_s^{1/2}$  due to independent information in  $N_s$  speckles. We also note that the SNR depends linearly on the binary separation. We recall here the SNR for parity detection using TC

$$\begin{aligned}
 \text{SNR}_{\text{TC/E}} &= \frac{4 \cdot 9^{1.5} M^{1/2} N_s^{1/2} \mathcal{N}_1 \mathcal{N}_2 (\mathcal{N}_1 - \mathcal{N}_2)}{3\sqrt{\pi} (2\mathcal{N}_1^3 + 7\mathcal{N}_1^2 \mathcal{N}_2 + 7\mathcal{N}_1 \mathcal{N}_2^2 + 2\mathcal{N}_2^3)} & (5.8) \\
 & \text{(section 5.3)} & (2.15) \\
 & \text{chapter 2)} & (4.33)
 \end{aligned}$$

where the numerical factor is provided by the field calculations given in the chapter 5 (otherwise the expression is the same as given in chapter 2). Note that the SNR improves with the diameter of the telescope. The TC method does not depend on the breakdown of the stationarity in the focal plane statistics. Thus every speckle in the PSF carries the parity information: this gives the factor  $N_s^{1/2}$  which increases linearly **with** the telescope diameter. We see that both KT and TC methods have an advantage and a disadvantage each. The KT method is second order and so intrinsically capable of beating the TC which is a third order method at sufficiently low flux levels. **However, the** TC method respects stationarity and thus wins a factor  $N_s^{1/2}$  over the KT method. We emphasise that this comparison is true for binary separations near the diffraction limit. For wider separation the KT improves. In the concluding chapter we present our numerical results for the SNR for parity detection using both these methods.

A discussion about the flux center. We have, throughout, assumed that the flux center is a given quantity. This is certainly not so. It is well known that the flux center for every frame wanders in the focal plane and significant improvement is possible **by**, centering all the frames. The reason for this centroid shift is attributed to the turbulence scales larger than the decorrelations length (especially scales of the telescope size or larger). These scales in the refractive index tilt the wavefront as a whole. The effect of these larger scales can be mimicked, however, by a larger value of  $\delta$ . This is for the following reason. Consider a frame of focal plane intensity. We can calculate the intensity double correlation for this. Now let us shift this image in the focal plane. The double correlation will also shift but the shift is along the  $45^\circ$  plane. Thus it can only increase the  $\delta$  and not diffuse the correlation ridges normal to their plane. This, of course, leads to a poorer SNR as the small parameter  $\frac{b}{\delta}$  becomes smaller. Beletik (1988)<sup>[11]</sup> in his numerical simulations finds the TC method to have better SNR than the KT method for complex sources. This he attributes to the wandering of the centroid. As we have argued this is indeed true. The wandering does make the KT method poorer but that is not the entire effect. The main reason why KT is poorer for complex sources is the fact that this method depends on stationarity breakdown crucially and has a small source size parameter in its SNR.

#### APPENDIX A4

The focal plane intensity due to a point source (the PSF) is



given by

$$R(x) = N_0 \left( \frac{k}{2\pi f} \right)^2 \int d\xi_1 d\xi_2 e^{i \frac{k}{f} x (\xi_1 - \xi_2)} \varphi(\xi_1) \varphi^*(\xi_2) e^{-\frac{\xi_1^2 + \xi_2^2}{2R^2}} \quad (4.34)$$

where  $N_0$  is normalization (see below),  $k = 2\pi/\lambda$ ,  $f$  is the focal length of the imaging system,  $\exp[-\{\xi_1^2 + \xi_2^2\}/2R^2]$  is apodization designed to give Gaussian beam if the pupil plane input fields were not corrupted by atmosphere. In the latter case  $\varphi(\xi_1) = 1$  for a point source at the origin and the PSF  $R_0(x)$  is given by

$$R_0(x) = N_0 \frac{k^2 R^2}{f^2} e^{-\frac{k^2 R^2 x^2}{f^2}} \quad (4.35)$$

The speckle diameter  $\rho$  is defined as area equivalent of the ideal PSF

$$\frac{1}{4} \pi \rho^2 = \int d^2 x e^{-\frac{k^2 R^2 x^2}{f^2}} \quad \text{or} \quad \rho = \frac{2f}{kR} \quad (4.36)$$

The normalization  $N_0$  is photon counts in an exposure per unit area due to a zeroth magnitude star i.e.

$$\int d^2 x R_0(x) = N_0 \pi R^2 \quad (4.37)$$

gives the total photon count in an exposure due to zeroth magnitude star (bandwidth taken into account) incident on a telescope of radius  $R$ . We assume that the pupil plane fields  $\varphi(\xi)$  due to atmospheric distortions are stationary Gaussian fields with two point correlation function

$$\langle \varphi(\xi_1) \varphi^*(\xi_2) \rangle = e^{-4(\xi_1 - \xi_2)^2 / \ell^2} \quad (4.38)$$

With this pupil plane field statistics the long exposure PSF is given by

$$\langle R(x) \rangle = \frac{N_0 k^2 \ell^2 R^2}{16 f^2} e^{-k^2 \ell^2 x^2 / 16 f^2} \quad (4.39)$$

The equivalent diameter of this seeing is given by

$$\frac{1}{4} \pi \sigma^2 = \int d^2x e^{-k^2 \ell^2 x^2 / 16 f^2} \quad \text{or} \quad \sigma = \frac{8f}{k\ell} \quad (4.40)$$

In this Gaussian model the average number of speckles  $N_s$  is

$$N_s = \frac{\sigma^2}{\rho^2} = 16 \frac{R^2}{\ell^2} \quad (4.41)$$

For example, if the seeing is 1" the decorrelation length defined by Eq 4.38 is 20 cm. This is purely due to the definition of the two point field correlation Eq 4.38. The general two point correlation can be obtained using Eq 4.38 and the well known pairing theorem for four point field correlation. The pairing theorem allows one to write a higher order correlation as a sum of products of double correlations. Consider  $N$  Gaussian random variable  $\psi_1, \dots, \psi_N$  and their conjugates  $\psi_1^*, \dots, \psi_N^*$ . Then form  $N$  distinct pairs out of these  $2N$  variables. Take the average of every pair. The average of the original  $2N$ -product is a sum of such paired products obtained in all possible ways. However, in speckle interferometry one can impose the further constraint that every pair must have one  $\psi_i$  and one  $\psi_j^*$ . Every path in the earth's atmosphere has a random optical path length of the order of hundreds of wavelengths. Therefore, the phase of  $\psi_1 \psi_2^*$  is completely random. The PSFDC is given by

$$\langle R(x)R(y) \rangle = \frac{1}{2^8} N_0^2 \frac{k^4 \ell^4 R^4}{f^4} \left\{ \underbrace{-\frac{k^2 \ell^2}{16 f^2} (x^2 + y^2)}_{\text{A term}} + \underbrace{e^{-\frac{k^2 R^2}{2 f^2} (x-y)^2} e^{-\frac{k^2 \ell^2}{32 f^2} (x+y)^2}}_{\text{B term}} \right\} \quad (4.42)$$

Now consider a binary with separation  $b$

$$S(x) = \alpha_1 \delta(x) + \alpha_2 \delta(x-b) \quad (4.43)$$

where we have chosen the focal plane origin to be the star 1. The coordinates of the flux center are  $\frac{\alpha_2}{\alpha_1 + \alpha_2} b$ . Since any asymmetry

in intensity double correlation is due to the binary separation we have chosen the first axis along the binary. The general two point correlation for the binary contains four PSF double correlations

$$\begin{aligned} \langle I(x)I(y) \rangle = & \alpha_1^2 \langle R(x)R(y) \rangle + \alpha_1 \alpha_2 \langle R(x-b)R(y) \rangle + \alpha_1 \alpha_2 \langle R(x)R(y-b) \rangle \\ & + \alpha_2^2 \langle R(x-b)R(y-b) \rangle \end{aligned} \quad (4.44)$$

This correlation is shown in Fig 4.2. Now consider the weight function of the first kind shown in Fig 4.3. This has three strips whose width is equal to the width of the feature B. Consider the central strip. It contains B features due to the first and the third basic PSF double correlation unit. In addition it also covers part of A features due to all the four units. The overlap of a A-feature and the weight function is equivalent to a B-feature as can be seen from Eq 4.42 and noting the fact that the width of the weight function is the same as that of a B-feature. The centers of the A-features due to the second and the fourth unit are off center but since we are dealing with small binary separations the overlap is nearly the same as that due to other units (the difference is in the third order in the binary separation). So the central strip contains six equivalent B features. Their centers and strengths are shown in Fig 4.3 which also shows contents of other strips. In this figure equivalent B features are primed and the subscript tells us the PSFDC unit which has generated it. It is possible to project the double correlation on the  $45^\circ$  line by integrating X , Y along  $-45^\circ$  line as the weight function chosen is independent of these coordinates. Let  $\eta = \frac{x_1 + y_1}{2}$  and  $\xi = \frac{x_1 - y_1}{2}$ . Integration can be

done for  $\xi$ . For an equivalent B-feature with **strength**  $\beta$  say and **center**  $\eta_c$  away from the jump in the weight function we can get the signal and the contribution to the variance as 1-d integrals along the  $45^\circ$  line

$$S = \frac{\pi^{1.5} N_0^2 k \ell^3 R^2 \beta}{2^{5.5} f} \int d\eta_1 \omega(\eta_1) e^{-\frac{k^2 \ell}{8f^2} (\eta_1 - \eta_c)^2} \quad (4.45)$$

$$V = \frac{\pi^{1.5} N_0^2 k \ell^3 R^2 \beta}{2^{4.5} f} \int d\eta_1 \omega^2(\eta_1) e^{-\frac{k^2 \ell^2}{8f^2} (\eta_1 - \eta_c)^2} \quad (4.46)$$

where  $\omega(\eta)$  is the weight along the  $45^\circ$  line. A representative of antisymmetric weight functions is shown in Fig 5.4c. This is a step function centered at the flux center. As shown in Fig 5.4c (which deals with similar case) the result of such a weight function on a B-feature is a contribution equivalent to the **central**  $\pm\eta_c$  part of the B-feature where  $\eta_c$  is the distance of the B-feature from jump in the weight function. So one has to note down the distances, from the jump, of all the effective B-feature contributing for all the three correlation ridges. For small binary separations the central part (the area between  $\pm\eta_c$ ) is well approximated by  $2\eta_c$  into the height of the feature. Note that  $\eta_c$  for all features is of the order of the binary separation.  $\omega^2(\eta)$  is unity everywhere. So doing the integrals in Eq 4.45 and Eq 4.46 we get the contribution to the signal and the variance by a typical B-feature with **strength**  $\beta$  and distance  $\eta_c$  from the jump in the weight function:

$$S = \frac{\pi^{1.5} N_0^2 k \ell^3 R^2 \beta \omega(\eta_c) |\eta_c|}{2^{4.5} f} \quad (4.47)$$

$$V = \frac{\pi^2}{2^3} N_0^2 \ell^2 R^2 \beta \quad (4.48)$$

In the expression Eq 4.47 the factor  $\omega(\eta_c)$  comes because depending

on which side of the  $-45^\circ$  line the center is the contribution is **+**ve or **-**ve. Note that both the signal and the noise are additive in features. This gives us the signal due to individual strips:

$$S_1 = S_3 = \frac{1}{2} S_2$$

$$S_2 = \frac{\pi^{1.5} N_0^2 k l^3 R^2 b \alpha_1 \alpha_2 (\alpha_1 - \alpha_2)}{2^{4.5} f(\alpha_1 + \alpha_2)}$$

The net signal is given by

$$S_{KT(B)} = \frac{\pi^{1.5} N_0^2 k l^3 R^2 b \alpha_1 \alpha_2 (\alpha_1 - \alpha_2)}{2^{3.5} f(\alpha_1 + \alpha_2)} \quad (4.49)$$

The variance calculation is trivial as the square of the weight function entering the expression for the variance is everywhere unity. We get

$$V_{KT(B)} = \frac{\pi^2}{2} N_0^2 l^2 R^2 (\alpha_1 + \alpha_2)^2 \quad (4.50)$$

This gives us the SNR for parity determination using double correlation for the weight function of the first kind.

$$SNR_{KT(B)} = \frac{4.9 M^{1/2} N_1 N_2 (N_1 - N_2)}{\sqrt{\pi} (N_1 + N_2)^2} \quad (4.12)$$

One can choose other antisymmetric weight functions instead of the step function but the results do not alter the scalings with  $N, b$

This is because the actual signal density along the  $45^\circ$  line is given by

$$S(\eta_1) \propto \eta_1 e^{-\frac{k^2 l^2}{8 f^2} \eta_1^2} \quad (4.51)$$

where  $\eta_1$  is the coordinate along the  $45^\circ$  line. We see that the signal comes from all over the seeing disk and one can not drastically improve the SNR by choosing any other weight function. Some fine tuning is, of course, possible. If the signal were coming from some localized part of the strip then one could

restrict the weight function to that part thus cutting down the noise from other regions which contributed little to the signal. In particular, for a linear weight function of the form  $w(\eta)=\eta$  the SNR is poorer by a factor  $\sqrt{\pi}$  .

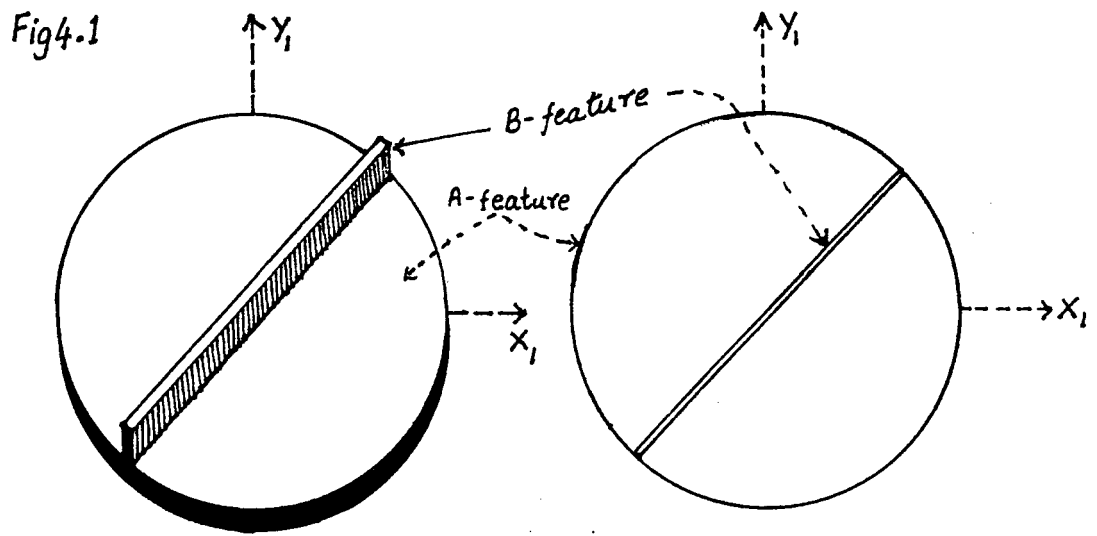


Fig 4.1 The PSF double correlation left: schematic; right: symbolic

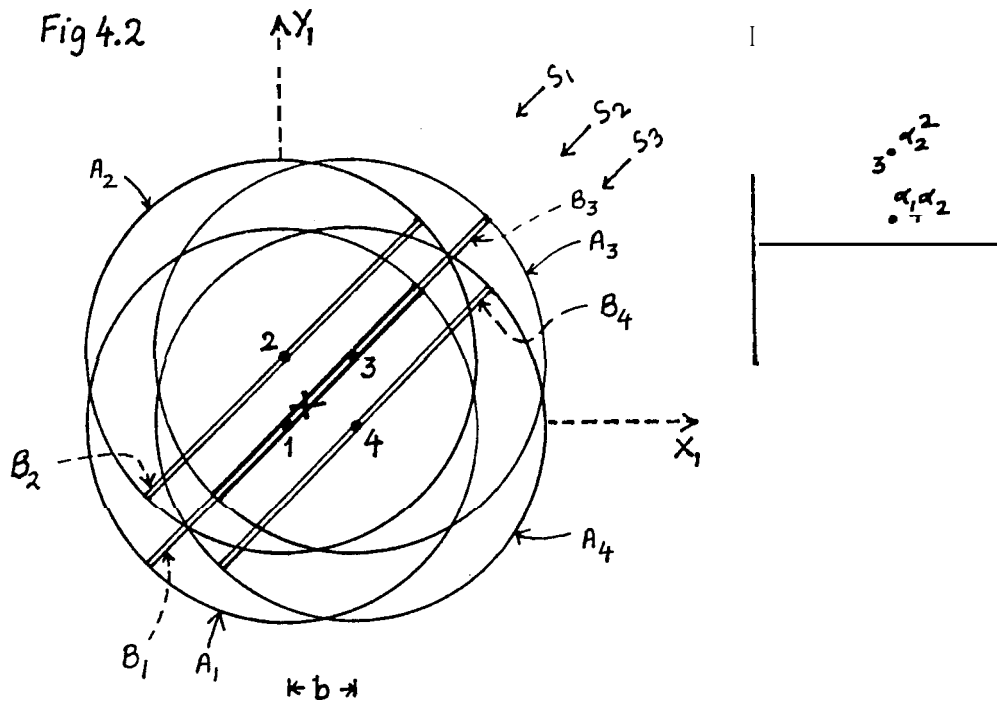


Fig 4.2 Double correlation for a binary. Inset: strengths of the four PSFDCs comprising binary double correlation.

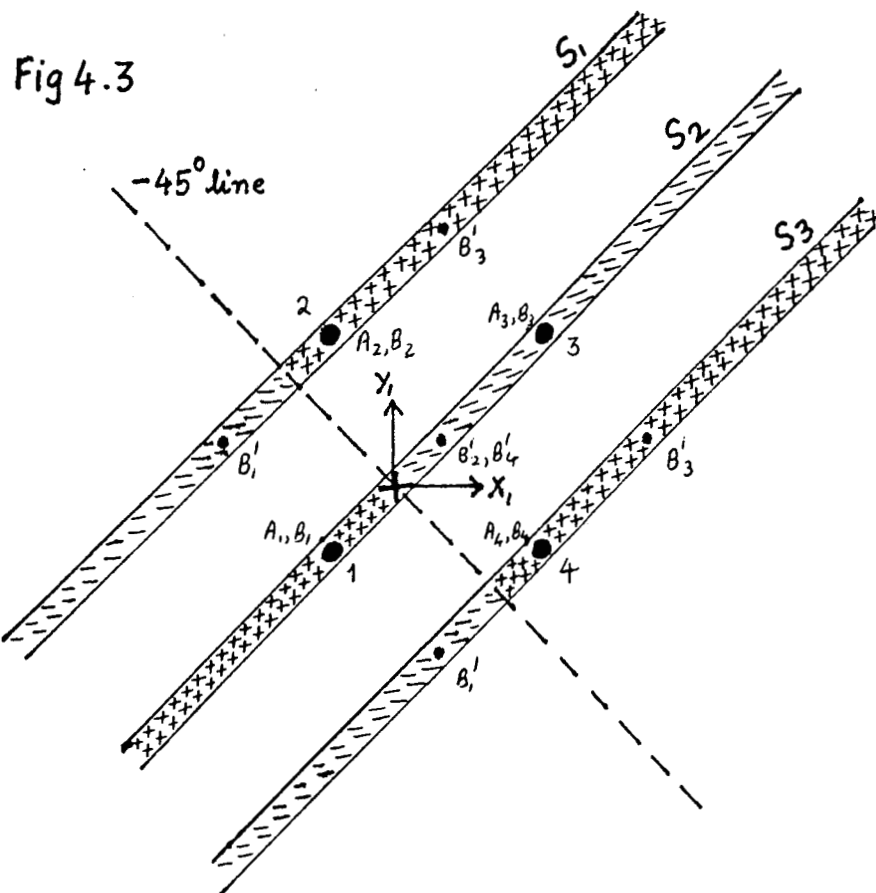


Fig 4.3. The weight function used to emphasise the B-feature

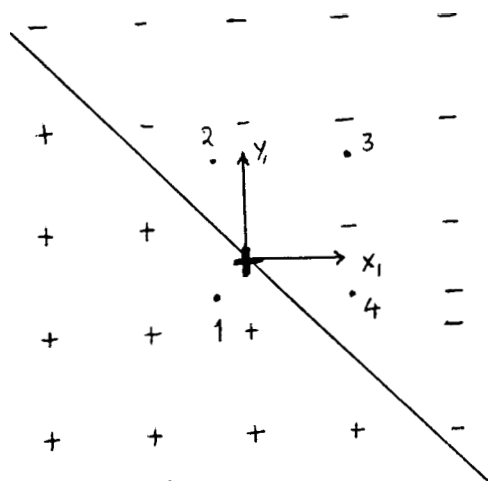


Fig 4.4

Fig 4.4. The weight function used to emphasise the feature A.